Synthesis and Electrochemistry of Iron(III) Corroles Containing a Nitrosyl Axial Ligand. Spectral Characterization of $[(OEC)Fe^{III}(NO)]^n$ Where n = 0, 1, 2, or −1 and OEC Is the Trianion of 2,3,7,8,12,13,17,18-Octaethylcorrole

Marie Autret,[†] Stefan Will,[‡] Eric Van Caemelbecke,[†] Johann Lex,[‡] Jean-Paul Gisselbrecht,[§] Maurice Gross,*[,§] Emanuel Vogel,*[,‡] and Karl M. Kadish*[,†]

Contribution from the Department of Chemistry, University of Houston, Houston, TX 77204-5641, Institut für Organische Chemie, Universität zu Köln, Greinstrasse 4, 50939 Köln, Germany, and Département de Chimie, URA CNRS 405, Université Louis Pasteur, 67000 Strasbourg, France

Received May 12, 1994[⊗]

Abstract: The synthesis, structural and spectral characterization of (OEC)Fe(NO) and $[(OEC)Fe(NO)]^+$ where OEC is the trianion of 2,3,7,8,12,13,17,18-octaethylcorrole, is reported. To our knowledge, $(OEC)Fe^{III}(NO)$ is the first example of a neutral air-stable iron(III) nitrosyl tetrapyrrole. It undergoes up to three oxidations and two reductions in nonaqueous media. The first two oxidations and both reductions are reversible and are located at $E_{1/2}$ = +0.61, +1.14, −0.41, and −1.92 V vs SCE in benzonitrile containing 0.1 M tetra-*n*-butylammonium perchlorate. The two oxidations involve the stepwise abstraction of a single electron from the corrole macrocycle and generate a stable iron(III) π-cation radical and dication, both of which still contain a coordinated NO axial ligand. The two one-electron reductions of $(OEC)Fe^{III}(NO)$ are also reversible and proceed without loss of the axial NO ligand. The first two oxidations and the first reduction of (OEC)Fe(NO) give products which are sufficiently stable to be spectroscopically characterized by UV–visible, IR, and/or ESR spectroscopy after *in situ* generation in PhCN or CH_2Cl_2. The ESR spectrum of the singly reduced product shows three g values at 2.00, 2.04, and 2.08 with nitric oxide ^{14}N hyperfine splitting in each region. This spectrum is quite similar to the one reported for five-coordinate $(TPP)Fe^{II}(NO)$ in toluene glass at 120 K and also resembles the spectra of various hemoproteins containing iron(II) with bound NO. This result is consistent with formation of a five-coordinate iron(II) macrocycle containing a bent MNO unit which is formulated as $[(OEC)Fe^{II}(NO)]^-$. The thin-layer FTIR spectral changes obtained during the first electroreduction are also consistent with formation of $[(OEC)Fe^{II}(NO)]^-$. The initial iron(III) compound has a ν_{NO} band at 1767 cm^{-1} in CH_2Cl_2 which disappears upon reduction as a new band diagnostic of a bent Fe(II)–NO unit grows in at 1585 cm^{-1}. The ESR and UV–visible spectral data of singly oxidized (OEC)Fe(NO) are also self-consistent and give clear evidence for formation of an iron(III) nitrosyl corrole π-cation radical rather than an iron(IV) nitrosyl corrole. The ESR spectrum of electrogenerated $[(OEC)Fe^{III}(NO)]^{\bullet+}$ in benzonitrile glass at 120 K has rhombic symmetry with resonances at g = 2.02, 2.00, 1.98 and is typical for a low-spin iron(III) species, i.e. $S = {}^1/_2$. This is the first example for the ESR characterization of an iron(III) tetrapyrrole π-cation radical. The ν_{NO} band of $[(OEC)Fe^{III}(NO)]^{\bullet+}$ is located at 1815 cm^{-1} which is 48 cm^{-1} higher than the ν_{NO} band of $(OEC)Fe^{III}(NO)$. X-ray crystallographic data shows that the neutral and singly oxidized corroles both contain a linear Fe–NO unit. It also indicates that the two corrole planes in $[(OEC)Fe(NO)]^+$ are close to each other and thus implies that the singly oxidized corrole is best formulated as an iron(III) π-cation radical rather than an iron(IV) nitrosyl.

Introduction

Studies of iron[1–28] and other transition metal[29–33]porphyrins containing one or two axially coordinated NO ligands have been carried out for over 20 years, but further intense investigations into the physicochemical properties and reactivity of compounds containing or interacting with this diatomic molecule have been stimulated by the recently discovered role of nitric oxide in several biological processes.[34–48] It was suggested that nitric oxide acts

[†] University of Houston.
[‡] Universität zu Köln.
[§] Université Louis Pasteur.
[⊗] Abstract published in *Advance ACS Abstracts*, August 15, 1994.

(1) Kon, H. *J. Biol. Chem.* **1968**, *243*, 4350.
(2) Wayland, B. B.; Olson, L. W. *J. Chem. Soc., Chem. Commun.* **1973**, 897.
(3) Wayland, B. B.; Olson, L. W. *J. Am. Chem Soc.* **1974**, *96*, 6037.
(4) Piciulo, P. L.; Rupprecht, G.; Scheidt, W. R. *J. Am. Chem. Soc.* **1974**, *96*, 5293.
(5) (a) Scheidt, W. R.; Frisse, M. E. *J. Am. Chem. Soc.* **1975**, *97*, 17. (b) Scheidt, W. R.; Brinegar, A. C.; Ferro, E. B.; Kirner, J. F. *J. Am. Chem. Soc.* **1977**, *99*, 7315.
(6) Perutz, M. F.; Kilmartin, J. V.; Nagai, K.; Szabo, A.; Simon, S. R. *Biochemistry* **1976**, *15*, 378.
(7) Scheidt, W. R.; Piciulo, P. L. *J. Am. Chem. Soc.* **1976**, *98*, 1913.
(8) Morse, R. H.; Chan, S. I. *J. Biol. Chem.* **1980**, *255*, 7876.
(9) Stevens, T. H.; Chan, S. I. *J. Biol. Chem.* **1981**, *256*, 1069.
(10) Olson, L. W.; Schaeper, D.; Lançon, D.; Kadish, K. M. *J. Am. Chem. Soc.* **1982**, *104*, 2042.
(11) Lançon, D.; Kadish, K. M. *J. Am. Chem. Soc.* **1983**, *105*, 5610.
(12) Palmer, G. In *Iron Porphyrins, Part II*; Lever, A. B. P., Gray, H. B., Eds.; Addison-Wesley Publishing Co.: Reading, MA, 1983; p 77.
(13) Fujita, E.; Fajer, J. *J. Am. Chem. Soc.* **1983**, *105*, 6743.
(14) Scheidt, W. R.; Lee, Y. J.; Hatano, K. *J. Am. Chem. Soc.* **1984**, *106*, 3191.
(15) Kadish, K. M.; Lançon, D.; Cocolios, P.; Guilard, R. *Inorg. Chem.* **1984**, *23*, 2372.
(16) Guilard, R.; Lagrange, G.; Tabard, A.; Lançon, D.; Kadish, K. M. *Inorg. Chem.* **1985**, *24*, 3649.
(17) (a) Barley, M. H.; Takeuchi, K.; Murphy, W. R., Jr.; Meyer, T. J. *J. Chem. Soc., Chem. Commun.* **1985**, 507. (b) Barley, M. H.; Takeuchi, K. J.; Meyer, T. J. *J. Am. Chem. Soc.* **1986**, *108*, 5876.
(18) Yoshimura, T. *Inorg. Chem.* **1986**, *25*, 688.
(19) Fernandes, J. B.; Feng, D.; Chang, A.; Keyser, A.; Ryan, M. D. *Inorg. Chem.* **1986**, *25*, 2606.
(20) Scheidt, W. R.; Lee, Y. J. *Struct. Bonding (Berlin)* **1987**, *64*, 1.
(21) Feng, D.; Ryan, M. D. *Inorg. Chem.* **1987**, *26*, 2480.
(22) Mu, X. H.; Kadish, K. M. *Inorg. Chem.* **1988**, *27*, 4720.
(23) Lin, X. Q.; Mu, X. H.; Kadish, K. M. *Electroanalysis* **1989**, *1*, 35.
(24) Mu, X. H.; Kadish, K. M. *Inorg. Chem.* **1990**, *29*, 1031.
(25) Finnegan, M. G.; Lappin, A. G.; Scheidt, W. R. *Inorg. Chem.* **1990**, *29*, 181.
(26) Choi, I.-K.; Liu, Y.; Feng, D.; Paeng, K.-J.; Ryan, M. D. *Inorg. Chem.* **1991**, *30*, 1832.

0002-7863/94/1516-9141$04.50/0

as a messenger which mediates the effect of the endothelium-derived relaxing factor in blood vessels[34-36] and the cytotoxic actions of macrophages.[37] Nitric oxide also plays a part in neuronal communication in the brain[38-41] where NO synthase (NOS) has a recognition site for arginine which is converted to NO and citrulline by a novel process which requires molecular oxygen.[42] Recent studies have also shown that there is a close similarity of the amino acid sequence between cytochrome P-450 reductase and NOS, suggesting that these two enzymes might have analogous functions.[43] Studies on CO binding to reduced NOS seem to confirm this analogy and suggest that NOS is a cytochrome P-450 type hemoprotein.[44,45] Electron transport in the enzymatic cycle involving conversion of nitrite to ammonia might occur via oxidized iron nitrosyl macrocycle transients,[49] and this underscores the importance of examining the spectroscopic and redox properties of high oxidation state iron nitrosyl porphyrins or porphyrin-like molecules.

Virtually all iron nitrosyl porphyrins and porphyrin-like macrocycles contain iron(II) in their neutral air-stable form. Electrochemical studies show that synthetic iron(II) nitrosyl porphyrins such as (TPP)Fe(NO) (TPP = the dianion of tetraphenylporphyrin) can undergo up to three reversible one-electron oxidations and two reversible one-electron reductions depending upon the solvent/supporting electrolyte system.[10,11,22,26] The first oxidation occurs at the metal center to generate an iron(III) nitrosyl complex which is stable on the voltammetric time scale, but the site of electron transfer can be shifted to the conjugated macrocycle for complexes of chlorins, bacteriochlorins, or isobacteriochlorins.[13]

Numerous singly oxidized iron nitrosyl complexes have been structurally[14] and/or spectroscopically[11,22,24] characterized, but other than the redox potentials,[22] almost nothing is known about the doubly or triply oxidized forms of these compounds. This is due in large part to the fact that electrogenerated complexes of $[(P)Fe(NO)]^n$, where P is the dianion of a given porphyrin ring and $n = +2$ or $+3$, are unstable and rapidly undergo loss and/or oxidation of the axial ligand.[11,22] Because of this instability, iron nitrosyl porphyrins or porphyrin-like macrocycles have yet to be spectroscopically or structurally characterized in high oxidation states. It is therefore not known whether such species would contain the positive charge localized on the macrocycle, on the metal center or on the NO axial ligand prior to decomposition.

This is examined in the present study which reports the synthesis and structural characterization of the first iron nitrosyl porphyrin-like macrocycle which contains a formal iron(III) center in its neutral air-stable form. The investigated compound is represented as (OEC)Fe(NO) where OEC is the trianion of 2,3,7,8,12,13,-17,18-octaethylcorrole. The deprotonated free base corrole

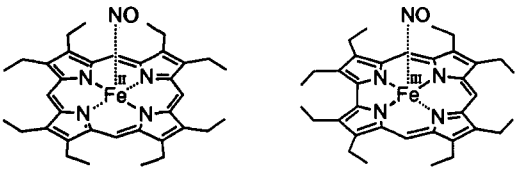

(OEP)Fe(NO) (OEC)Fe(NO)

(labeled in its general form as "C") has a −3 charge as compared to −2 in the case of the related porphyrins, and this leads to stable $(C)M^{III}$ (M = Co[50,51]), $[(C)M^{IV}]^+$ (M = Fe[52]), and $(C)M^{V}O$ (M = Cr[53]) derivatives rather than to the lower metal oxidation state $(P)M^{II}$ (M = Co) and $[(P)M^{III}]^+$ (M = Fe or Cr) compounds seen in the case of metalloporphyrins.[54]

For example, $(OEC)Fe(C_6H_5)$, (OEC)FeCl, and $[(OEC)Fe]_2O$ have all been characterized as containing an iron(IV) metal ion[52] and each can undergo up to three one-electron oxidations in nonaqueous media leading, in some cases, to compounds containing a formal iron(V) oxidation state.[55] It is therefore of special interest to know whether singly oxidized (OEC)Fe will exist in an Fe(IV) oxidation state when coordinated by other types of axial ligands and specifically whether an iron(IV) or even an iron(V) nitrosyl corrole might be obtained upon the electrooxidation of $(OEC)Fe^{III}(NO)$ in nonaqueous media. This is investigated in the present paper which examines each redox reaction of $(OEC)Fe^{III}(NO)$ by thin-layer UV–visible and/or FTIR spectroelectrochemistry. The singly oxidized and singly reduced species are also characterized by EPR spectroscopy after bulk oxidation or bulk reduction and, when combined with the UV–visible and IR data, provide the first comparative study of an iron nitrosyl tetrapyrrolic macrocycle in four different oxidation states. Finally, the neutral and singly oxidized compounds are structurally characterized, thus enabling comparisons not only between the structural and IR data of $[(OEC)Fe(NO)]^n$ ($n = 0$ or 1+) but also between iron nitrosyl corroles in different oxidation states and the related and well-studied iron nitrosyl porphyrins.

Experimental Section

Chemicals. Benzonitrile (PhCN) was purchased from Aldrich Chemical Co. and distilled over P_2O_5 under vacuum prior to use. Absolute dichloromethane (CH_2Cl_2) over molecular sieve, obtained from Fluka Chemical Co., was used without further purification. $CDCl_3$, used for NMR measurements, was purchased from Aldrich Chemical Co. and used without further purification. Tetra-*n*-butylammonium perchlorate (TBAP) was purchased from Sigma Chemical Co., recrystallized from ethyl alcohol and dried under vacuum at 40 °C for at least 1 week prior to use. Tetra-*n*-butylammonium hexafluorophosphate ($TBAPF_6$) (electrochemical grade), from Fluka, was used as received.

(27) Traylor, T. G.; Magde, D.; Marsters, J.; Jongeward, K.; Wu, G.-Z.; Walda, K. *J. Am. Chem. Soc.* **1993**, *115*, 4808.
(28) Hoshino, M.; Ozawa, K.; Seki, H.; Ford, P. C. *J. Am. Chem. Soc.* **1993**, *115*, 9568.
(29) (a) Scheidt, W. R.; Hatano, K.; Rupprecht, G. A.; Piciulo, P. L. *Inorg. Chem.* **1979**, *18*, 292. (b) Scheidt, W. R.; Hoard, J. L. *J. Am. Chem. Soc.* **1973**, *95*, 8281.
(30) Kelly, S. L.; Kadish, K. M. *Inorg. Chem.* **1984**, *23*, 679.
(31) Fujita, E.; Chang, C. K.; Fajer, J. *J. Am. Chem. Soc.* **1985**, *107*, 7665.
(32) Kadish, K. M.; Mu, X. H.; Lin, X. Q. *Inorg. Chem.* **1988**, *27*, 1489.
(33) Hu, S. *Inorg. Chem.* **1993**, *32*, 1081.
(34) Furchgott, R. F.; Vanhoutte, P. M. *FASEB J.* **1989**, *3*, 2007.
(35) Moncada, S.; Palmer, R. M. J.; Higgs, E. A. *Biochem. Pharmacol.* **1989**, *38*, 1709.
(36) Ignarro, L. J. *Annu. Rev. Pharmacol. Toxicol.* **1990**, *30*, 535.
(37) Hibbs, J. B., Jr; Vavrin, Z.; Traintor, R. R. *J. Immunol.* **1987**, *138*, 550.
(38) Bredt, D. S.; Snyder, S. H. *Proc. Nat. Acad. Sci. U.S.A.* **1989**, *86*, 9030.
(39) Garthwaite, J.; Garthwaite, G.; Palmer, R. M. J.; Moncada; S. *Eur. J. Pharmacol.* **1989**, *172*, 413.
(40) Solomon, H. S. *Science* **1992**, *257*, 494.
(41) Zhang, J.; Dawson, V. L.; Dawson, T. M.; Snyder, S. H. *Science* **1994**, *263*, 687.
(42) Kwon, N. S.; Nathan, C. F.; Gilker, C.; Griffith, O. W.; Matthews, D. E.; Stuehr, D. J. *J. Biol. Chem.* **1990**, *265*, 13442.
(43) Bredt, D. S.; Hwang, P. M.; Glatt, C. E.; Lowenstein, C.; Reed, R. R.; Snyder, S. H. *Nature* **1991**, *351*, 714.
(44) White, K. A.; Marletta, M. A. *Biochemistry* **1992**, *31*, 6627.
(45) Mc Millan, K.; Bredt, D. S.; Hirsch, D. J.; Snyder, S. H.; Clark, J. E.; Masters, B. S. S. *Proc. Nat. Acad. Sci. U.S.A.* **1992**, *89*, 11141.
(46) Lipton, S. A; Choi, Y.; Pan, Z.; Lei, S. Z.; Chen, H. V.; Sucher, N. J.; Loscalzo, J.; Singel, D. J.; Stamler, J. S. *Nature* **1993**, *364*, 626.
(47) Stamler, J. S; Singel, D. J.; Loscalzo, J. *Science* **1992**, *258*, 1898.
(48) Malinski, T.; Tcha, Z. *Nature* **1992**, *358*, 676.
(49) Ozawa, S.; Fujii, H.; Morishima, I. *J. Am. Chem. Soc.* **1992**, *114*, 1548.
(50) Conlon, M.; Johnson, A. W.; Overend, W. R.; Rajapaksa, D.; Elson, C. M. *J. Chem. Soc., Perkin Trans. 1* **1973**, 2281.
(51) Murakami, Y.; Yamada, S.; Matsuda, Y.; Sakata, K. *Bull. Chem. Soc. Jpn.* **1978**, *51*, 123.
(52) Vogel, E.; Will, S.; Schulze Tilling, A.; Neumann, L.; Lex, J.; Bill, E.; Trautwein, A. X.; Wieghardt, K. *Angew. Chem.* **1994**, *106*, 771; *Angew. Chem., Int. Ed. Engl.* **1994**, *33*, 731.
(53) Matsuda, Y.; Yamada, S.; Murakami, Y. *Inorg. Chim. Acta* **1980**, *44*, L309.
(54) Buchler, J. W. In *The Porphyrins*; Dolphin, D.; Ed.; Academic Press: New York, 1978; Vol. I, Part A, Chapter 10.
(55) Van Caemelbecke, E.; Will, S.; Autret, M.; Gisselbrecht, J.-P.; Gross, M.; Vogel, E.; Kadish, K. M. Manuscript in preparation.

Instrumentation. ^{1}H and ^{13}C NMR spectra were recorded at 300 and 75.5 MHz, respectively, on a Bruker AP 300 NMR spectrometer at 298 K. The solvent signals were used as a standard at δ = 7.24 ppm (^{1}H) or δ = 77.0 ppm (^{13}C) and signal assignments were made by inverse ^{1}H–^{13}C correlation experiments.[56] ESR spectra were recorded at 120 K on an IBM ER 100D spectrometer equipped with an ER 040-X microwave bridge and an ER 080 power supply or at 77K on a Bruker ESP 380E spectrometer. The *g* values were measured with respect to diphenylpicrylhydrazyl (g = 2.0036 ± 0.0003).

UV–visible spectra were recorded on a Perkin-Elmer Lambda 7 spectrophotometer with a 1 cm quartz cell while IR measurements were performed with a Perkin-Elmer Series 1600, a Perkin-Elmer IR spectrophotometer 283, or an IBM Model 32 FTIR spectrophotometer. Infrared spectroelectrochemical measurements were made under nitrogen with an IBM IR 32 FTIR spectrometer using a specially constructed light-transparent three-electrode cell.[23] UV–visible spectroelectrochemical experiments were performed with a platinum thin-layer electrode.[57] Potentials for both the IR and UV–visible spectroelectrochemical measurements were applied and monitored with an EG&G Model 173 potentiostat. Time-resolved UV–visible spectra were recorded with a Tracor Northern Model 6500 rapid scan spectrophotometer/multichannel analyzer.

Cyclic voltammetry was carried out with an EG&G Model 173 potentiostat or an IBM Model EC 225 voltammetric analyzer. Current–voltage curves were recorded on an EG&G Princeton Applied Research Model RE-0151 X-Y recorder. A three electrode system was used and consisted of a glassy carbon or platinum button working electrode, a platinum wire counter electrode and a saturated calomel reference electrode (SCE). This reference electrode was separated from the bulk solution by a fritted-glass bridge filled with the solvent/supporting electrolyte mixture. All potentials are referenced to the SCE.

RDE measurements were carried out on a computerized multipurpose electrochemical device (DACFAMOV-MICROTEC, Toulouse, France) connected to a microcomputer (APPLE II). The working electrode was a 2 mm diameter platinum disk and the reference an aqueous Ag/AgCl electrode which was separated from the solution by a glass frit of low porosity. Under these conditions ferrocene was oxidized at +0.37 V vs Ag/AgCl in CH_2Cl_2, 0.1 M TBAP. The available potential range was from −1.70 to +1.90 V vs Ag/AgCl or −1.65 to +1.94 V vs SCE.

Mass spectral measurements were made with a Finnigan H-SQ 30 using 3-nitrobenzyl alcohol as the matrix. Elemental analyses were performed by Bayer AG in Leverkusen.

Syntheses of (OEC)Fe(NO). The title compound was synthesized from (OEC)Fe(py),[52] (OEC)FeCl,[52] or (OEC)H_3[58] by one of three different methods, all three of which resulted in the same final (OEC)Fe(NO) product.

method A:

$$(OEC)Fe(py) \xrightarrow{NO} (OEC)Fe(NO) \qquad 84\%\ \text{yield}$$

method B:

$$(OEC)FeCl \xrightarrow{NaNO_2} (OEC)Fe(NO) \qquad 58\%\ \text{yield}$$

method C:

$$(OEC)H_3 \xrightarrow[2.\ NaNO_2]{1.\ FeCl_2} (OEC)Fe(NO) \qquad 85\%\ \text{yield}$$

Method A. A stirred solution of 131 mg (0.2 mmol) of pyridine-(2,3,7,8,12,13,17,18-octaethylcorrolato)iron(III), (OEC)Fe(py),[52] in 25 mL of dichloromethane containing a few drops of pyridine was saturated with argon. Nitric oxide was introduced into the solution for 5 min, whereupon the color changed from brown to red. The volatile compounds were removed *in vacuo* and the residue was then purified by passing it through a column of alumina (ICN, activity II) using dichloromethane as eluant. After recrystallization from hexane, the nitrosyl compound was obtained as brown needles (102 mg, 84%) which decomposed above 210 °C.

(56) Bax, A.; Subramanian, S. *J. Magn. Reson.* **1986**, *67*, 565.
(57) Lin, X. Q.; Kadish, K. M. *Anal. Chem.* **1985**, *57*, 1498.

Table 1. Crystallographic Data for (OEC)Fe(NO)·C_6H_6 and [(OEC)Fe(NO)]$FeCl_4$·1.5CH_2Cl_2

	(OEC)Fe(NO)·C_6H_6	[(OEC)Fe(NO)]$FeCl_4$·1.5CH_2Cl_2
chemical formula	$C_{41}H_{49}FeN_5O$	$C_{35}H_{43}N_5OFe_2Cl_4$·1.5CH_2Cl_2
formula weight	683.70	930.63
space group	triclinic/$P\bar{1}$	tetragonal/$P4_12_12$
Z	2	8
a, Å	10.477(3)	13.263(3)
b, Å	12.063(3)	13.263(3)
c, Å	15.226(3)	49.493(10)
β, deg	85.67(2)	90
V, Å^3	1845.5	8706(3)
data: unique/observed [$F_o^2 > 2\sigma(F_o^2)$]	6244/5311	5237/3435
no. of parameters	531	637
R1 (F_o^2)[a]	0.0788	0.0717
wR2 (F_o^2)[b]	0.2008	0.2168

[a] $R1 = [\sum||F_o| - |F_c||]/[\sum|F_o|]$. [b] $\{[\sum w(F_o^2 - F_c^2)^2]/[\sum w(F_o^2)^2]\}^{1/2}$.

Method B. A solution of 122 mg (0.2 mmol) of chloro(2,3,7,8,12,-13,17, 18-octaethylcorrolato)iron(IV), (OEC)FeCl,[52] in 25 mL of dichloromethane was stirred vigorously with 1 mL of a saturated aqueous sodium nitrite solution for 2 h. The organic layer was washed with water and dried over sodium sulfate, and the solvent was evaporated *in vacuo*. The residue was chromatographed on alumina (ICN, activity II), using dichloromethane as eluant. The first red fraction was collected and evaporated to dryness. Recrystallization of the product obtained from hexane yielded 70 mg (58%) of (OEC)Fe(NO).

Method C. A solution of 523 mg of free base 2,3,7,8,12,13,17,18-octaethylcorrole, (OEC)H_3[58] (1 mmol), and 0.6 *g* (3 mmol) of ferrous chloride tetrahydrate in 15 mL pyridine/methanol (1:2) was refluxed for 30 min. During this period the color changed from purple to brown. Subsequently, 1 mL of a saturated sodium nitrite solution was added dropwise to the hot solution. After addition of 40 mL of methanol at room temperature, the precipitated (OEC)Fe(NO) was collected by filtration and washed with methanol and water. The nitrosyl compound was purified by passing through a column of alumina (ICN activity II) using dichloromethane as eluant. (OEC)Fe(NO) was recovered in brown needles after recrystallization from hexane (515 mg, 85%).

^{1}H NMR ($CDCl_3$, 300 MHz): δ (ppm) = 7.39 (singlet, 2H; H-5,15), 7.34 (singlet, 1H; H-10), 3.19 (multiplet, 4H; H-2a,18a), 3.15 (multiplet, 4H; H-3a,17a), 2.94 (multiplet, 4H; H-7a,13a), 2.91 (multiplet, 4H; H-8a,12a), 1.40 (triplet, 4H; H-3b,17b), 1.35 (triplet, 4H; H-2b,18b), 1.31 (triplet, 4H; H-7b,13b), 1.30 (triplet, 4H; H-8b,12b). ^{13}C NMR ($CDCl_3$, 75.5 MHz): δ (ppm) = 146.85 (C-1,19), 145.54 (C-6,14), 143.41 (C-9,11), 137.40 (C-4,16), 137.10 (C-3,17), 136.54 (C-7,13), 135.42 (C-8,12), 131.50 (C-2,18), 110.88 (C-10, $^1J_{CH}$ = 154 Hz), 109.54 (C-5,15, $^1J_{CH}$ = 153 Hz), 19.73 (C-2a,18a), 18.63 (C-3a,17a), 18.39 (C-7a,13a), 18.19 (C-8a,12a), 17.53 (C-3b,17b), 17.19 (C-2b,18b), 16.89 (C-8b,12b), 16.55 (C-7b,13b). MS (FAB/NBA): m/z 575 (100) [M − NO]$^+$, 560 (12) [M − NO − CH_3·]$^+$, 545 (20) [M − NO − 2CH_3·]$^+$, 530 (10) [M − NO − 3CH_3·]$^+$. IR (CsI): ν (cm^{-1}) = 2963, 2930, 2869, 1758(ν_{NO}), 1580, 1548, 1532, 1489, 1449, 1376, 1349, 1308, 1276, 1212, 1158, 1134, 1083, 1057, 1011, 959, 911, 878. UV–vis (CH_2Cl_2): λ_{max} (nm) (ϵ, mol^{-1} l cm^{-1}) = 275 (19 200) sh, 308 (20 500) sh, 334 (35 800) sh, 373 (70 800), 535 (15 200), 820 nm (810). Elemental analysis calculated for $C_{35}H_{43}N_5FeO$: C, 69.42; H, 7.16; N, 11.56. Found: C, 69.45; H, 7.45; N, 11.50.

X-ray Structural Determination of (OEC)Fe(NO). Single crystals of (OEC)Fe(NO)·C_6H_6 were grown by slow evaporation of a benzene solution of (OEC)Fe(NO). A crystal of dimensions 0.50 × 0.45 × 0.25 mm was sealed in a Lindemann glass capillary and X-ray data were collected on an Enraf-Nonius CAD4 diffractometer using monochromated Mo Kα radiation. Experimental conditions are given in Table 1. Cell parameters were determined by least-squares refinement of 25 reflections. The intensities of two standard reflections were checked during data collection every 2 hours. The structure was solved by direct methods (MolEN[59]) and refined for all observed reflections with $F_0^2 > 2\sigma F_0^2$ (non-hydrogen atoms with anisotropic, hydrogen atoms with isotropic

(58) Murakami, Y.; Matsuda, Y.; Sakata, K.; Yamada, S.; Tanaka, Y.; Aoyama, Y. *Bull. Chem. Soc. Jpn.* **1981**, *54*, 163.
(59) MolEN, an interactive structure solution procedure, Enraf-Nonius, Delft, The Netherlands.

Table 2. Selected Bond Lengths (Å) for (OEC)Fe(NO)[a]

Fe–N(5)	1.631(3)	C(3)–C(4)	1.448(5)
Fe–N(4)	1.896(3)	C(4)–C(5)	1.364(5)
Fe–N(1)	1.897(3)	C(5)–C(6)	1.406(5)
Fe–N(2)	1.922(3)	C(6)–C(7)	1.438(5)
Fe–N(3)	1.921(3)	C(7)–C(8)	1.370(5)
O–N(5)	1.171(4)	C(8)–C(9)	1.417(5)
N(1)–C(1)	1.352(4)	C(8)–C(26)	1.507(6)
N(1)–C(4)	1.384(5)	C(9)–C(10)	1.389(5)
N(2)–C(6)	1.375(4)	C(10)–C(11)	1.395(5)
N(2)–C(9)	1.393(4)	C(11)–C(12)	1.428(5)
N(3)–C(14)	1.380(4)	C(12)–C(13)	1.359(5)
N(3)–C(11)	1.395(5)	C(13)–C(14)	1.443(5)
N(4)–C(19)	1.354(5)	C(14)–C(15)	1.402(5)
N(4)–C(16)	1.378(5)	C(15)–C(16)	1.388(6)
C(1)–C(19)	1.434(6)	C(16)–C(17)	1.429(5)
C(1)–C(2)	1.442(6)	C(17)–C(18)	1.379(6)
C(2)–C(3)	1.375(6)	C(18)–C(19)	1.425(6)

[a] Only values for the corrole framework are given. Numbers in parentheses are estimated standard deviations in the least significant digit.

Table 3. Selected Bond Angles (deg) for (OEC)Fe(NO)[a]

N(5)–Fe–N(4)	106.44(14)	C(5)–C(6)–C(7)	125.9(3)
N(5)–Fe–N(1)	106.0(2)	C(8)–C(7)–C(6)	107.1(3)
N(4)–Fe–N(1)	78.10(13)	C(7)–C(8)–C(9)	106.9(3)
N(5)–Fe–N(2)	102.69(14)	C(10)–C(9)–N(2)	122.4(3)
N(4)–Fe–N(2)	150.15(11)	C(10)–C(9)–C(8)	127.1(3)
N(1)–Fe–N(2)	87.85(12)	N(2)–C(9)–C(8)	110.5(3)
N(5)–Fe–N(3)	102.28(14)	C(9)–C(10)–C(11)	126.6(3)
N(4)–Fe–N(3)	88.00(13)	C(10)–C(11)–N(3)	122.6(3)
N(1)–Fe–N(3)	151.00(13)	C(10)–C(11)–C(12)	127.2(3)
N(2)–Fe–N(3)	92.13(12)	N(3)–C(11)–C(12)	110.1(3)
C(1)–N(1)–C(4)	109.3(3)	C(13)–C(12)–C(11)	106.9(3)
C(1)–N(1)–Fe	119.1(2)	C(12)–C(13)–C(14)	107.7(3)
C(4)–N(1)–Fe	130.0(2)	N(3)–C(14)–C(15)	123.8(3)
C(6)–N(2)–C(9)	105.5(3)	N(3)–C(14)–C(13)	109.4(3)
C(6)–N(2)–Fe	126.8(2)	C(15)–C(14)–C(13)	126.6(3)
C(9)–N(2)–Fe	126.5(2)	C(16)–C(15)–C(14)	123.5(3)
C(14)–N(3)–C(11)	105.9(3)	N(4)–C(16)–C(15)	120.6(3)
C(14)–N(3)–Fe	126.7(2)	N(4)–C(16)–C(17)	108.2(3)
C(11)–N(3)–Fe	125.8(2)	C(15)–C(16)–C(17)	131.1(4)
C(19)–N(4)–C(16)	108.9(3)	C(18)–C(17)–C(16)	106.8(4)
C(19)–N(4)–Fe	118.9(3)	C(17)–C(18)–C(19)	107.7(3)
C(16)–N(4)–Fe	131.0(2)	N(4)–C(19)–C(18)	108.5(3)
O–N(5)–Fe	176.9(3)	N(4)–C(19)–C(1)	110.8(3)
N(1)–C(1)–C(19)	110.5(3)	C(18)–C(19)–C(1)	140.7(3)
N(1)–C(1)–C(2)	108.1(3)		
C(19)–C(1)–C(2)	141.4(3)		
C(3)–C(2)–C(1)	108.2(3)		
C(2)–C(3)–C(4)	106.3(3)		
C(5)–C(4)–N(1)	121.0(3)		
C(5)–C(4)–C(3)	130.7(3)		
N(1)–C(4)–C(3)	108.1(3)		
C(4)–C(5)–C(6)	123.5(3)		
N(2)–C(6)–C(5)	124.1(3)		
N(2)–C(6)–C(7)	109.9(3)		

[a] Only values for the corrole framework are given. Numbers in parentheses are estimated standard deviations in the least significant digit.

temperature factors) using the SHELXL-93 program package.[60] Hydrogen atom parameters of the methyl groups were idealized (C–H = 0.96 Å, H–C–H = 109.5°). Due to its diffuse electron density maxima, the benzene molecule was treated as a regular hexagon with a variable C–C bond length during refinement with hydrogen atoms placed on idealized positions (C–H = 0.93 Å, C–C–H = 120°). A final difference electron density map exhibited some peaks near the iron atom (maximum height 1.55 e A^{-3}) but was otherwise featureless. Main bond distances and angles for (OEC)Fe(NO) are given in Tables 2 and 3 while Figure 1 presents a view of the (OEC)Fe(NO) complex.

Synthesis of [(OEC)Fe(NO)]$^{+}$. Nitrosyl(2,3,7,8,12,13,17,18-octaethylcorrolato)iron, (OEC)Fe(NO), 303 mg (0.5 mmol), was refluxed with 1.5 g of finely grounded ferric chloride hexahydrate in 20 mL dichloromethane for 20 min. The solution was then filtered over sodium

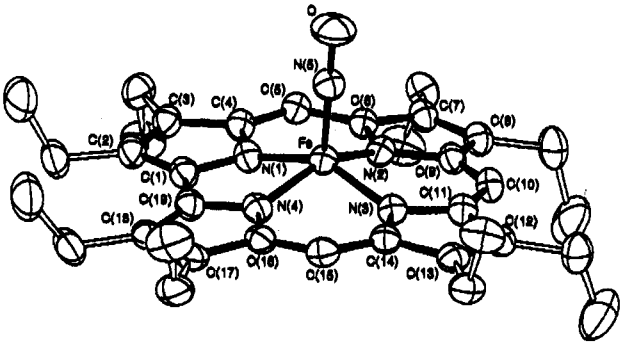

Figure 1. ORTEP diagram of (OEC)Fe(NO) (perspective view, hydrogen atoms omitted) displaying the atom labeling scheme for the core atoms used in Tables 2 and 3. Ellipsoids are contoured at the 50% probability level.

sulfate and concentrated to a volume of 1 mL by heating. The oxidized compound was allowed to crystallize for 4 h at 4 °C. The obtained black shiny octahedra of [(OEC)Fe(NO)]$^{+}$FeCl$_4^-$·1.5 CH_2Cl_2 were washed successively with cold dichloromethane and pentane and recrystallized from dichloromethane: yield 305 mg (66%); density : 1.430 g cm^{-3}. Elemental analysis calculated for $C_{35}H_{43}N_5OFe_2Cl_4$·1.5 CH_2Cl_2 (C, 47.11; H, 4.98; N, 7.53; Cl, 26.67) and calculated for $C_{35}H_{43}N_5OFe_2Cl_4$ (C, 52.33; H, 5.40; N, 8.72; Cl, 17.65); found: C, 51.66; H, 5.31; N, 8.60; Cl, 18.04. These data indicate a nearly complete solvent loss. UV–vis [CH_2Cl_2, ϵ in mol^{-1} L cm^{-1} calculated for [(OEC)Fe(NO)]$^{+}$FeCl$_4^-$·1.5(CH_2Cl_2)]: λ_{max} (ϵ) = 240 (33 800), 335 (57 900), 365 (67 500), 478 (9 200) sh, 554 (4 500) sh, 609 (4 100) nm. IR (CsI): ν (cm^{-1}) = 2971, 2934, 2873, 1809 (ν_{NO}), 1497, 1464, 1451, 1376, 1357, 1324, 1298, 1213, 1130, 1117, 1107, 1056, 1010, 963, 866, 373 (ν_{FeCl}).

X-ray Structural Determination of [(OEC)Fe(NO)]$^{+}$. Single crystals of [(OEC)Fe(NO)]$^{+}$FeCl$_4^-$·1.5CH_2Cl_2 were obtained by reaction of (OEC)Fe(NO) in CH_2Cl_2 with an excess of ferric chloride hexahydrate for 20 min followed by a slow evaporation of the filtered solution. Cell determination and data collection procedures are as described for (OEC)-Fe(NO). The dimension of the unit cell and the systematic extinctions suggest a tetragonal crystal system. The structure was solved with SHELX-86[61] assuming the space group $P4_12_12$. During subsequent cycles of difference Fourier synthesis, it became evident that two crystallographically independent molecules of dichloromethane are present. One of them is placed on a crystallographic mirror plane so that a stochiometry of [(OEC)Fe(NO)]$^{+}$FeCl$_4^-$·1.5CH_2Cl_2 is obtained. In the final model, all non-hydrogen atoms were refined with anisotropic, hydrogen atoms with isotropic temperature factors using SHELXL-93.[60] Due to the observed density, ρ_{obs} = 1.434 g cm^{-1}, the occupancy factors of the solvent molecules were chosen as one (ρ_{calc} = 1.420 g cm^{-1}). The final difference Fourier electron map shows that there are no electron peaks and holes larger than 0.951 and –0.652 e A^{-3}, respectively.

Results

Synthesis and Spectral Characterization. The synthesis of (OEC)Fe(NO) was carried out as described in the Experimental Section. The nitrosyl complex, (OEC)Fe(NO), was prepared by a ligand exchange reaction. Treatment of (OEC)Fe(py)[52] with nitric oxide immediately yields (OEC)Fe(NO) in a smooth reaction. (OEC)Fe(NO) is stable in the solid state, in solution, or even in neat pyridine where no formation of the pyridine complex, (OEC)Fe(py), is observed. The high stability of (OEC)-Fe(NO) and tendency for its formation is also confirmed by the fact that the same nitrosyl compound is formed as a main product in a reaction between the chloroiron(IV) corrole, (OEC)FeCl,[52] and nitrite ions, analogous to what is observed in the porphyrin series.[25] The remarkable stability of (OEC)Fe(NO) distinguishes the iron nitrosyl corrole from its transition metal counterparts in the porphyrin series, i.e., [(P)Fe(NO)]$^{+}$ [14,22] and (P)Mn(NO),[29a,62] both of which have a d^5 metal center and are rather unstable compounds.

(60) Sheldrick, G. M. SHELXL-93 *J. Appl. Crystallogr.* **1994**, in preparation.

(61) Sheldrick, G. M. *Acta Crystallogr. Sect. A* **1990**, *46*, 467.

(62) Wayland, B. B.; Olson, L. W.; Siddiqui, Z. U. *J. Am. Chem. Soc.* **1976**, *98*, 94.

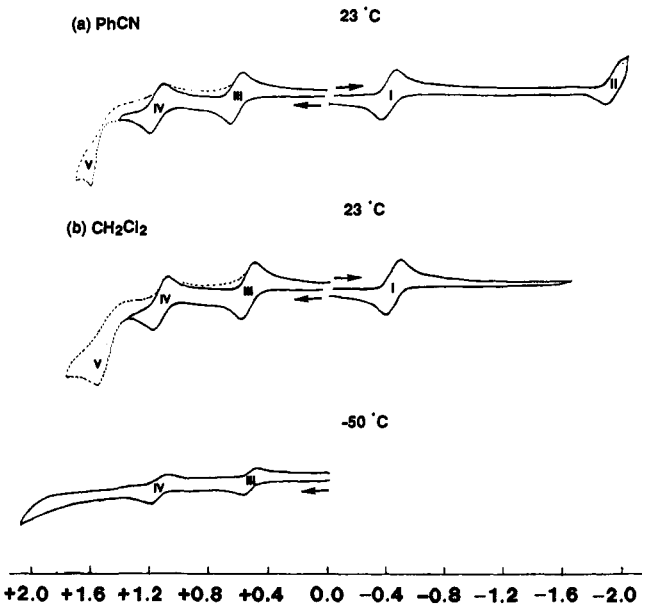

Figure 2. Cyclic voltammograms of (OEC)Fe^{III}(NO) in (a) PhCN and (b) CH_2Cl_2 containing 0.1 M TBAP. Scan rate = 0.1 V/s.

The ^{1}H NMR spectrum of (OEC)Fe(NO) shows sharp resonances, characteristic of a diamagnetic compound. The *meso* protons H-5,15 and H-10 occur as singlets at δ = 7.39 and 7.34, respectively, whereas the ethyl groups give rise to resonances in the range of δ = 3.19–2.91 (CH_2) and δ = 1.40–1.30 (CH_3). (OEC)Fe(NO) shows, as compared to the free base ligand,[52] an upfield shift of all resonances, which is most pronounced for the *meso* protons (about 2 ppm). Similar shifts (but more pronounced) are also observed in the case of the μ-oxo dimer [(OEC)Fe]$_2$O.[52] The observed upfield shift indicates a considerable electronic interaction between the FeNO unit and the π-electron system of the corrole ligand leading to a decreased diamagnetic ring current in (OEC)Fe(NO). Thus the corrole macrocycle has to be considered as noninnocent[63] in (OEC)Fe(NO). The ^{13}C NMR spectrum exhibits the expected 18 signals and confirms the close relationship between [(OEC)Fe]$_2$O[52] and (OEC)Fe(NO) because the resonances of the corresponding carbon atoms of the ring macrocycle are observed at similar fields.[52]

No molecular ion was detected in the mass spectrum of (OEC)Fe(NO), even using FAB, and the main peak in the spectrum is [(OEC)Fe]$^+$ at m/z = 575. The infrared spectrum of (OEC)Fe(NO) in the solid state is dominated by the strong NO vibration at 1758 cm^{-1} while its UV–visible spectrum in dichloromethane is characteristic of porphyrinoids[64] in that it shows a Soret-like absorption at 373 nm [ϵ = 70 800 L/(mol cm)] and a less intense band in the visible region, at 535 nm [ϵ = 15 200 L/(mol cm)].

Electrochemistry. Cyclic voltammograms of (OEC)Fe^{III}(NO) in PhCN and CH_2Cl_2 containing 0.1 M TBAP are shown in Figure 2. In these two solvents the compound undergoes up to two reversible one-electron reductions (processes I and II), two reversible one-electron oxidations (processes III and IV), and a third oxidation (process V) which is chemically irreversible at room temperature and not observed in CH_2Cl_2 at –50 °C. The RDE voltammogram in CH_2Cl_2 (not shown) has three well-defined steps of similar height and each occurs at a potential close to the $E_{1/2}$ measured by cyclic voltammetry for processes I, III, and IV in the same solvent. The RDE data indicates that the same number of electrons is involved in the reduction process I as in the oxidation processes III and IV. These three reactions were each investigated by thin-layer UV–visible and/or IR spectroelectrochemistry as well as by ESR spectroscopy after bulk electrolysis at a controlled potential.

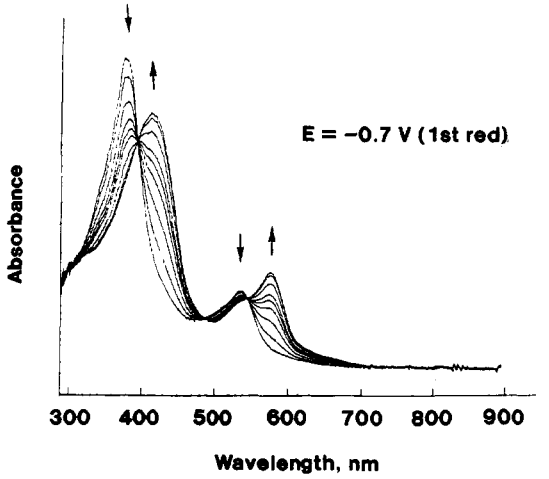

Figure 3. Thin-layer spectral changes obtained upon conversion of (OEC)Fe^{III}(NO) to [(OEC)Fe^{II}(NO)]$^-$ in PhCN, 0.2 M TBAP, by controlled-potential reduction at –0.7 V.

Table 4. Spectral Data of [(OEC)Fe(NO)]^n (n = 0, +1, or –1)

species	λ_{max}, nm[a] ($\epsilon \times 10^{-3}$, L/(mol cm))	ν_{NO}[b] (cm^{-1})	ESR[c] g values
[(OEC)Fe^{III}(NO)]$^{\cdot+}$	371 (47.1)	1815	2.02 2.00 1.98
(OEC)Fe^{III}(NO)	376 (61.2), 536 (13.0)	1767	silent
[(OEC)Fe^{II}(NO)]$^-$	412 (50.2), 538 (12.2), 577 (17.7)	1585	2.08 2.04 2.00

[a] In PhCN, 0.2 M TBAP. [b] In CH_2Cl_2, 0.2 M TBAP. [c] Values for [(OEC)Fe^{II}(NO)]$^-$ are in PhCN at 120 K while those for [(OEC)Fe^{III}(NO)]$^{\cdot+}$ are in CH_2Cl_2 at 77 K.

Electroreduction. The two reductions of (OEC)Fe(NO) occur at $E_{1/2}$ = –0.41 and –1.92 V in PhCN. The peak to peak potential separations, $\Delta E_p = |E_{pc} - E_{pa}|$, are 80 mV at a scan rate of 0.1 V/s and the anodic to cathodic peak current ratios, i_{pa}/i_{pc}, are close to unity at this scan rate, both of which indicate diffusion-controlled one-electron transfers. The reversibility of processes I and II suggests that the NO axial ligand remains bound to the iron center after reduction on the cyclic voltammetry time scale and this would lead to the stepwise formation of [(OEC)Fe(NO)]$^-$ and [(OEC)Fe(NO)]$^{2-}$ as the first two corrole reduction products in solution. The facile first reduction of (OEC)Fe^{III}(NO) occurs at a potential similar to that for the Co(III)/Co(II) reaction of (OMC)Co(PPh$_3$)[65] and this suggests that the first electron is added to the metal center of (OEC)Fe(NO) to generate [(OEC)Fe^{II}(NO)]$^-$. This assignment is also consistent with UV–visible, IR, and ESR spectroscopic data of the singly reduced product as discussed in the following paragraphs.

Time-dependent electronic absorption spectra taken during controlled-potential electroreduction of (OEC)Fe^{III}(NO) in PhCN, 0.2 M TBAP at –0.7 V are shown in Figure 3. The UV–visible spectrum of the initial complex has a Soret band at 376 nm and a single visible band at 536 nm, both of which shift toward higher wavelengths upon electroreduction (see Table 4). Isosbestic points are seen at 390 and 550 nm, indicating the lack of spectral intermediates upon conversion of (OEC)Fe^{III}(NO) to [(OEC)Fe^{II}(NO)]$^-$. These spectral changes are reversible and the UV–visible spectrum of (OEC)Fe^{III}(NO) could be fully regenerated by controlled-potential reoxidation at 0.0 V. The same results are obtained upon electroreduction of (OEC)Fe-

(63) Anson, F. C.; Collins, T. J.; Richmond, T. G.; Santarsiero, B. D.; Toth, J. E.; Treco, B. G. R. T. *J. Am. Chem. Soc.* **1987**, *109*, 2974.
(64) Gouterman, M. In *The Porphyrins*; Dolphin, D., Ed.; Academic Press: New York, 1978; Vol. III, Part A, Chapter 1.
(65) Kadish, K. M.; Koh, W.; Tagliatesta, P.; Sazou, D.; Paolesse, R.; Licoccia, S.; Boschi, T. *Inorg. Chem.* **1992**, *31*, 2305.

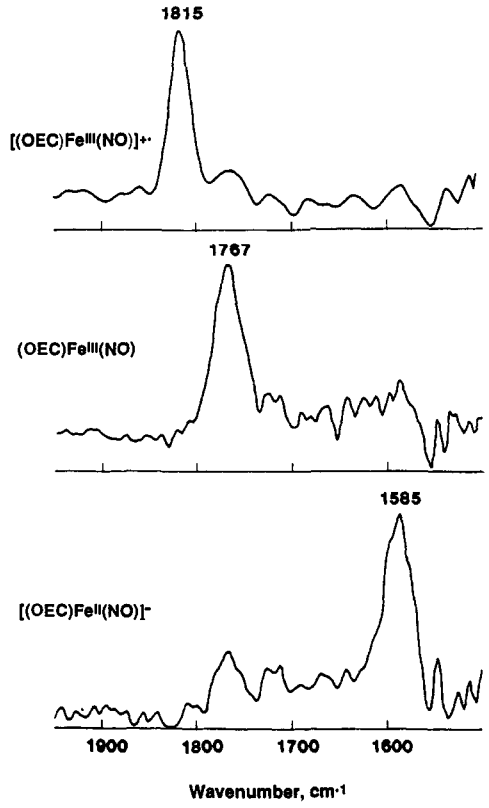

Figure 4. IR spectra of [(OEC)Fe^{III}(NO)]^n in CH_2Cl_2, 0.2 M TBAP, where n = +1, 0, −1.

Table 5. NO Vibration Frequencies (cm^{-1}) of (P)M^{II}(NO), [(P)M^{II}(NO)]$^{+\cdot}$ and (P)M^{III}(NO) Complexes (M = Fe, Co, Mn, or Cr)

metal, M	ligand, P	conditions[a]	ν_{NO}, cm^{-1} M^{II}	M^{II}(rad)[b]	M^{III}	$\Delta\nu_{NO}$	ref
Fe	OEC	CH_2Cl_2	1585		1767	182	*d*
	OEP	CH_2Cl_2	1667		1854	187	22
	TMP	CH_2Cl_2	1672		1838	166	22
	TPP	CH_2Cl_2	1678		1848	170	22
	OEChl	Nujol	1670	1705		35	13
	OEiBC	Nujol	1670	1680		10	13
Co	TPP	CH_2Cl_2	1684	1726		42	29b
	OEP	Nujol	1660	1700		40	31
	MeOEChl	Nujol	1660	1700		40	31
	2,3-DMeOEiBC	Nujol	1655	1695		40	31
Mn	TPP	Nujol	1760		1830[c]	70	29a
Cr	TPP	Nujol	1700				29a

[a] CH_2Cl_2 solutions contain 0.1 M tetra-*n*-butylammonium perchlorate as supporting electrolyte. [b] M^{II}(rad) represents the π-cation radical of the metal(II) nitrosyl complex. [c] M^{III} is also coordinated to a chloride axial ligand. [d] This work.

(NO) in CH_2Cl_2, 0.1 M $TBAPF_6$. This spectral reversibility, as well as the presence of isosbestic points, is consistent with the reversible electrochemistry of the (OEC)Fe(NO)/[(OEC)Fe(NO)]$^-$ process and gives further evidence that the NO axial ligand remains coordinated to the iron center after the first electroreduction and formation of the Fe(II) derivative.

Thin-layer FTIR spectroscopic changes obtained during the first electroreduction of (OEC)Fe^{III}(NO) are also consistent with formation of [(OEC)Fe^{II}(NO)]$^-$. The 1767 cm^{-1} NO band of the initial iron(III) compound disappears upon reduction in CH_2Cl_2 as a new band grows in at 1585 cm^{-1} (see Figure 4 and Table 4). The NO vibration frequencies for neutral and singly reduced (OEC)Fe(NO) are also given in Table 5 which lists ν_{NO} values for selected complexes of (P)M^{II}(NO), [(P)M^{II}(NO)]$^{+\cdot}$ and (P)M^{III}(NO) where M = Fe, Co, Mn, or Cr. As seen in this table, the 182 cm^{-1} difference in ν_{NO} between (OEC)Fe(NO)

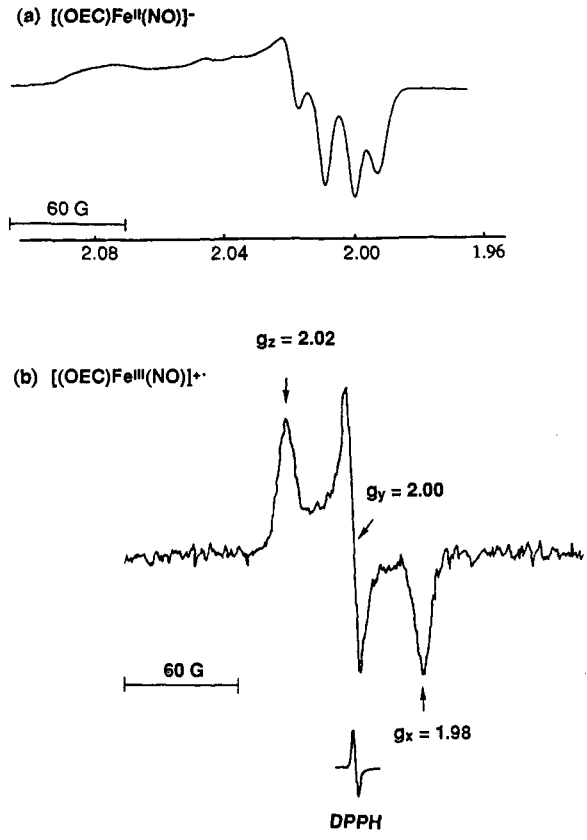

Figure 5. ESR spectra of electrogenerated (a) [(OEC)Fe^{II}(NO)]$^-$ in CH_2Cl_2 at 77K and (b) [(OEC)Fe^{III}(NO)]$^{+\cdot}$ in PhCN at 120 K.

and its singly reduced product falls in a range of values (170–187 cm^{-1}) observed upon the electrochemical conversion of [(P)Fe^{III}(NO)]$^+$ to (P)Fe^{II}(NO) where P represents the dianion of octaethylporphyrin (OEP), tetramesitylporphyrin (TMP) or tetraphenylporphyrin (TPP).

Additional evidence for the formation of an Fe^{II}–NO complex in [(OEC)Fe(NO)]$^-$ is given by the ESR spectrum obtained in CH_2Cl_2 glass at 77 K after bulk controlled-potential reduction of (OEC)Fe(NO) at −0.7 V (Figure 5a). This spectrum shows three g values with nitric oxide ^{14}N hyperfine splitting in each region (see Table 4 and Figure 5a). It is quite similar to the ESR spectrum reported for five coordinate (TPP)Fe^{II}(NO) in toluene glass at 120 K[3] and also resembles the spectra for various hemoproteins containing iron(II) with bound NO.[12] However, many hemoproteins containing a NO axial ligand usually show a nine-line ESR spectrum rather than a pronounced hyperfine triplet. These nine lines are due to the presence of an additional nitrogenous base as a sixth axial ligand.[12]

Electrooxidation. The first two oxidations of (OEC)Fe^{III}(NO) in PhCN, 0.1 M TBAP occur at $E_{1/2}$ = 0.61 and 1.14 V. The peak to peak separations are both about 80 mV at a scan rate of 0.1 V/s and the ratio of cathodic to anodic peak currents are close to unity under the same experimental conditions. These results indicate that both oxidations involve diffusion-controlled one-electron transfers. In contrast, the third oxidation is irreversible in that it is accompanied by a fast chemical reaction, as shown by the absence of a cathodic peak coupled to the anodic one in process V and the decrease in cathodic rereduction currents for processes III and IV under these experimental conditions (see dashed line in Figure 2). The third oxidation disappears at low temperature or fast scan rates. This suggests that the peak V arises from an irreversible process, the rate of which is slower at low temperature leading to an anodic peak which shifts and broadens to become undetectable at low temperature or high scan rate.

The UV–visible changes obtained upon thin-layer controlled-potential oxidation of (OEC)Fe^{III}(NO) in PhCN, 0.2 M TBAP

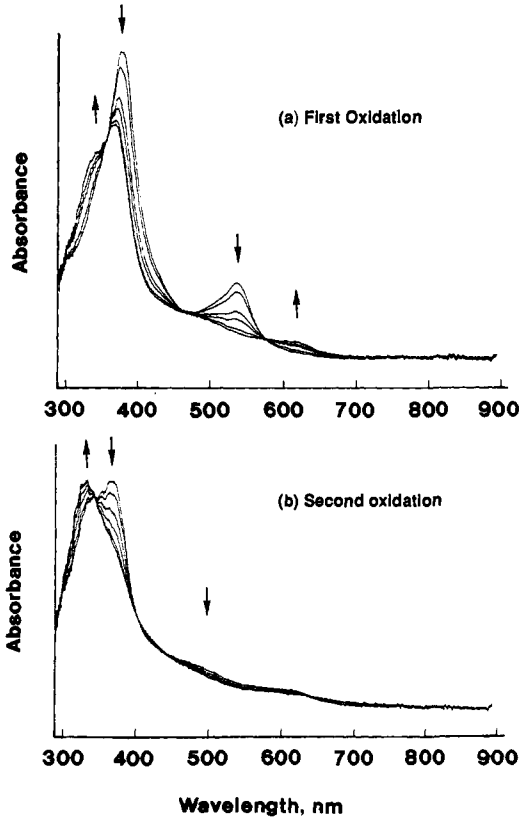

Figure 6. Thin-layer spectral changes obtained upon the stepwise conversion of (a) $(OEC)Fe^{III}(NO)$ to $[(OEC)Fe^{III}(NO)]^{\bullet+}$ at an applied potential of 0.8 V and (b) $[(OEC)Fe^{III}(NO)]^{\bullet+}$ to $[(OEC)Fe^{III}(NO)]^{2+}$ at an applied potential of 1.3 V, in PhCN, 0.2 M TBAP.

at +0.8 V are shown in Figure 6a. These spectral changes are reversible, and the initial spectrum of $(OEC)Fe^{III}(NO)$ could be fully recovered by applying a controlled potential of 0.0 V after electrooxidation. The 376 nm Soret band of $(OEC)Fe^{III}(NO)$ blue shifts and decreases in intensity during the first one-electron oxidation while the visible band at 536 nm vanishes as a weak new absorption grows in at *ca.* 610 nm. Isosbestic points are observed at 470 and 575 nm. The spectrum of the singly oxidized species has a split Soret band with a maximum at 371 nm and a shoulder at 342 nm. Similar spectral changes are also observed when the thin-layer controlled potential oxidation is carried out at +0.7 V in CH_2Cl_2, 0.1 M $TBAPF_6$. The weak band at 610 nm in Figure 6a might suggest the formation of a corrole π-cation radical[65-67] but a weak absorption above 600 nm is also seen for Fe(IV) corroles with other axial ligands.[52] On the other hand, the conclusions resulting from analysis of ESR and IR spectra of electrogenerated $[(OEC)Fe(NO)]^+$ (see later sections) are quite definitive and clearly indicate the formation of a corrole π-cation radical.

The IR spectrum of electrogenerated $[(OEC)Fe^{III}(NO)]^{\bullet+}$ in CH_2Cl_2, 0.2 M TBAP, is shown in Figure 4 which also gives the spectrum of the neutral and singly reduced compounds under the same solution conditions. The same IR spectrum could be obtained for $[(OEC)Fe^{III}(NO)]^{\bullet+}$ by either FTIR thin-layer spectroelectrochemistry or by bulk controlled-potential electrolysis of $(OEC)Fe^{III}(NO)$ at +0.8 V in CH_2Cl_2, 0.2 M TBAP. This indicates a quite stable Fe^{III}–NO π-cation radical in solution and also enables a characterization of the species by X-ray crystallography (see later sections).

The shift of ν_{NO} from 1767 cm^{-1} for $(OEC)Fe^{III}(NO)$ to 1815 cm^{-1} for $[(OEC)Fe^{III}(NO)]^{\bullet+}$ is consistent with the data obtained by UV–visible spectroscopy in that it suggests formation of a corrole π-cation radical rather than an iron(IV) nitrosyl derivative. The small, 40 cm^{-1}, shift in ν_{NO} between the two compounds (see Table 5) suggests a macrocycle centered oxidation and this is also the conclusion which results from the ESR and Mössbauer[68] data that gives further evidence for formation of a corrole π cation radical upon abstraction of one electron from $(OEC)Fe^{III}(NO)$.

The ESR spectrum of electrogenerated $[(OEC)Fe^{III}(NO)]^{\bullet+}$ in benzonitrile glass at 120 K (Figure 5b) has rhombic symmetry with resonances at g = 2.02, 2.00, 1.98 and is typical for a low-spin iron(III) species, (i.e., $S = {}^1/_2$).[71-73] This EPR spectrum seems to rule out formation of $[(OEC)Fe^{IV}(NO)]^+$ as an oxidation product of $(OEC)Fe^{III}(NO)$. Indeed, if the first oxidation were to occur at the metal center to give $[(OEC)Fe^{IV}(NO)]^+$, the resulting ESR spectrum should be quite similar to the one of $(OEC)Fe^{II}(NO)$ (Figure 5a), since only one unpaired electron would be located on the NO axial ligand. This is clearly not the case.

The one-electron oxidation of electrogenerated $[(OEC)Fe^{III}(NO)]^{\bullet+}$ occurs at $E_{1/2}$ = 1.14 V. The UV–visible spectrum shows a further blue shift in the Soret band and the final spectrum of $[(OEC)Fe(NO)]^{2+}$ (Figure 6b) has only a single absorption band at 333 nm. This spectrum is quite similar to the spectrum of doubly oxidized $(OMC)Co(PPh_3)$ which also has a single band at 333 nm in PhCN and has been characterized as a dication.[65] Once again, the UV–visible spectral changes are reversible and the spectrum of the original $(OEC)Fe^{III}(NO)$ derivative could be totally recovered by switching the controlled-potential back to 0.0 V. Unfortunately, the doubly oxidized compound is unstable on time scales longer than cyclic voltammetry, and all attempts to characterize the NO band of electrogenerated $[(OEC)Fe(NO)]^{2+}$ by IR spectroscopy were unsuccessful. However, the data obtained by UV–visible, IR, and ESR spectroscopy are self-consistent and indicate formation of a stable Fe(III) π-cation radical and an unstable dication after the first and second one-electron oxidations of $(OEC)Fe^{III}(NO)$.

Discussion

The iron nitrosyl corrole exists in the crystal as pairs of partly overlapping cofacial molecules with frameworks laterally shifted by 4.2 Å. The interactions of the two (OEC)Fe(NO) units are distinctly weaker (interplanar distance 3.6–3.7 Å; iron–iron distance 6.32 Å) than those in $[(OEP)Fe(NO)]ClO_4$ which forms a tight π–π dimer[14] (interplanar distance 3.36 Å; iron–iron distance 4.24 Å).

The iron atom is five-coordinate with the nitrosyl group in the apical position of a distorted tetragonal pyramid. The metal atom in (OEC)Fe(NO) is displaced by 0.470 Å from the mean plane of the four pyrrole nitrogen atoms. The corrole framework exhibits a domed conformation due to the alignment of the N-donor atoms toward the metal center (the maximum distance of a carbon and nitrogen atom from the mean plane of the corrole framework is 0.203 Å). Relevant bond lengths, distances, and angles are given in Tables 2, 3, and 7 respectively.

(66) Phillippi, M. A.; Goff, H. M. *J. Am. Chem. Soc.* **1982**, *104*, 6026.
(67) Fuhrhop, J.-H.; Mauzerall, D. *J. Am. Chem. Soc.* **1969**, *91*, 4174.
(68) The Mössbauer spectrum of (OEC)Fe(NO)[69] (δ = 0.01 mm s^{-1}, ΔE_q = 1.81 mm s^{-1}, 135 K) is very similar to that of $[(OEC)Fe(NO)]^+FeCl_4^-$ (δ = 0.00 mm s^{-1}, ΔE_q = 1.98 mm s^{-1}, 120 K), suggesting that the ionic species has been oxidized at the corrole macrocycle rather than at the metal and that both nitrosyl compounds contain an Fe(III) center. The two nitrosyl complexes exhibit isomer shifts δ and quadrupole splittings ΔE_q that favorably compare with those of other iron(III) nitrosyl complexes with trianionic ligands.[70]
(69) Bill, E. Private communication, Institut für Physik, Medizinische Universität Lübeck, Germany.
(70) Gerbeleu, N. V.; Arion, V. B.; Simonov, Y. A.; Zavodnik, V. E.; Stavrov, S. S.; Turta, K. I.; Gradinaru, D. I.; Birca, M. S.; Pasynskii, A. A.; Ellert, O. *Inorg. Chim. Acta* **1992**, *20*, 173.
(71) Otsuka, T.; Ohya, T.; Sato, M. *Inorg. Chem.* **1985**, *24*, 776.
(72) Ogoshi, H.; Sugimoto, H.; Yoshida, Z.-I.; Kobayashi, H.; Sakai, H.; Maeda, Y. *J. Organomet. Chem.* **1982**, *234*, 185.
(73) Tabard, A.; Cocolios, P.; Lagrange, G.; Gerardin, R.; Hubsch, J.; Lecomte, C.; Zarembowitch, J.; Guilard, R. *Inorg. Chem.* **1988**, *27*, 110.

Table 6. Comparison of Structural Parameters for Porphyrin and Corrole Nitrosyl Complexes with d^5, d^6, and d^7 Metal Ions

d electrons	compound[a]	M–NO, Å	N–O, Å	M–N–O, deg	ref
d^5	(OEC)Fe^{III}(NO)	1.631(3)	1.171(4)	176.9(3)	*c*
	[(OEC)Fe^{III}(NO)]$FeCl_4$	1.655(10)	1.115(12)	171.4(9)	*c*
	[(OEP)Fe^{III}(NO)]ClO_4	1.644(3)	1.112(4)	176.9(3)	14
	[(TPP)Fe^{III}(NO)(H_2O)]ClO_4	1.652(5)	1.150[b]	174.4(10)	14
	(TTP)Mn^{II}(NO)	1.641(2)	1.160(3)	177.8(3)	29a
d^6	(TPP)Fe^{II}(NO)	1.717(7)	1.122(12)	149.2(6)	5a
d^7	(TPP)Co^{II}(NO)	1.833(53)	1.01(2)	135.2(8)	29b

[a] OEC is the trianion of octaethylcorrole; OEP, TTP, and TPP are the dianions of octaethyl-, tetra-*p*-tolyl-, and tetraphenylporphyrin, respectively. [b] The NO ligand was treated as a rigid group with a fixed bond length during refinement. [c] This work.

Table 7. Comparison of Structural Parameters of (OEC)Fe(NO) and $[(OEC)Fe(NO)]^{\bullet+}$

	(OEC)Fe(NO)	$[(OEC)Fe(NO)]^{\bullet+}$
Fe–NO, Å	1.631(3)	1.655(10)
N–O, Å	1.171(4)	1.115(12)
Fe–N–O, deg	176.9(3)	171.4(9)
Fe–N,[a] Å	1.909(3)	1.912(8)
C_α–C_β,[a] Å	1.434(5)	1.462(14)
C_β–C_β,[a] Å	1.371(5)	1.365(20)
ΔN_4,[b] Å	0.470(1)	0.406(5)
Δ(core),[c] Å	0.556(1)	0.371(2)
Δ(C,N),[d] Å	0.203(3)	0.106(9)

[a] Average values. [b] Distance of the iron atom from the mean plane of the four pyrrole nitrogen atoms. [c] Distance of the iron atom from the mean plane of the 23-atom corrole core. [d] Maximum distance of a C, N atom from the mean plane of the 23-atom corrole core.

Structural parameters of the FeNO unit are typical for those observed in nitrosyl metalloporphyrins containing a d^5 metal ion (see Table 6). The nitrosyl ligand is coordinated in a nearly linear fashion (M–N–O = 176.9°) and this is according to theoretical results which predict a linear arrangement for an $\{FeNO\}^6$ unit.[74,75] The observed coordination geometry distinguishes (OEC)Fe(NO) significantly from those nitrosyl complexes which contain an iron(II) or cobalt(II) central metal ion and exhibit a bent M–NO moiety with a considerably longer M–NO bond (see Table 6). The Fe–NO bond in (OEC)Fe(NO) is short (1.631 Å), indicating a stronger back-bonding interaction from the metal to the NO ligand. In agreement with this electron transfer, there is an elongation of the NO bond (1.171 Å) with respect to the bond length in NO^+ (1.06 Å). The electron transfer from the metal to the nitrosyl ligand in (OEC)Fe(NO) seems to be the most pronounced among nitrosyl metalloporphyrins containing d^5 metals due to the fact that (OEC)Fe(NO) exhibits the shortest Fe–NO bond and the longest N–O distance.

The Fe–N distances in (OEC)Fe(NO) (average value 1.909 Å) are similar to those for several iron(IV) corroles[52] (average values 1.871–1.906 Å), while the distance of the iron atom from the N_4 plane is slightly longer in (OEC)Fe(NO) (0.470 vs 0.272–0.422 Å). However, the Fe–N distances in (OEC)Fe(NO), which contains a low-spin iron(III), are distinctly shorter than those in low-spin iron(III) porphyrins (average values 1.96–2.02 Å).[20] The bond lengths are therefore influenced by the macrocycle ligand as well as by the oxidation state of the metal.

The electrochemical measurements indicate that four different iron nitrosyl corroles can be generated from the initial (OEC)-Fe^{III}(NO) species as shown in eqs 1–4, where the listed potentials are measured in PhCN. Three of these, $[(OEC)Fe(NO)]^-$, $[(OEC)Fe(NO)]^{\bullet+}$, and $[(OEC)Fe(NO)]^{2+}$, are sufficiently stable to be spectroscopically characterized by UV–visible, IR and/or ESR spectroscopy after *in situ* generation in PhCN or CH_2Cl_2.

$$(OEC)Fe^{III}(NO) + e^- \rightleftarrows [(OEC)Fe^{II}(NO)]^- \quad E_{1/2} = -0.41\ V \quad (1)$$

$$[(OEC)Fe^{II}(NO)]^- + e^- \rightleftarrows [(OEC)Fe(NO)]^{2-} \quad E_{1/2} = -1.92\ V \quad (2)$$

$$(OEC)Fe^{III}(NO) \rightleftarrows [(OEC)Fe^{III}(NO)]^{\bullet+} + e^- \quad E_{1/2} = +0.61\ V \quad (3)$$

$$[(OEC)Fe^{III}(NO)]^{\bullet+} \rightleftarrows [(OEC)Fe(NO)]^{2+} + e^- \quad E_{1/2} = +1.14\ V \quad (4)$$

The ν_{NO} values for neutral and singly reduced (OEC)Fe^{III}-(NO) are summarized in Table 5 along with literature values for related synthetic macrocycles containing four different transition metals in a +2 or +3 oxidation state. The values of ν_{NO} for these species range from 1660 to 1854 cm^{-1} depending upon the type of macrocycle, the specific central metal ion and its oxidation state, the charge on the overall complex, and the geometry of the MNO unit. Whether the MNO unit is linear or bent depends on the number of metal d electrons and metal coordination number. According to Walsh diagrams, metal nitrosyl complexes with a coordination number of five have a bent MNO unit when M is a d^6 or d^7 metal and a linear unit when M is a d^5 metal.[74,75] This has previously been demonstrated for (TPP)Fe^{II}(NO)[3] and (TPP)-Co^{II}(NO)[29b] which contain d^6 and d^7 metal ions, respectively, and have a bent MNO unit as compared to (TTP)Mn^{II}(NO)[29a] and $[(OEP)Fe^{III}(NO)]^+$,[14] both of which have d^5 metal ions and a linear MNO unit.

The investigated (OEC)Fe^{III}(NO) derivative is isoelectronic with both $[(P)Fe^{III}(NO)]^+$ and (P)Mn(NO). It has a linear Fe–NO unit as shown by the X-ray data described above. The Fe–NO band is located at 1767 cm^{-1} which is 87 cm^{-1} lower than that of singly charged $[(OEP)Fe^{III}(NO)]^+$ (see Table 5) and this difference in ν_{NO} can be accounted for by the different charges on the two iron(III) complexes. The basicity of OEC is also higher than that of the other macrocycles for compounds listed in Table 5, and this brings about a stronger equatorial ligand field which will also contribute to an increased electron density at the metal center, leading to a lower NO vibration frequency.

The ν_{NO} value of the singly reduced iron(II) corrole, $[(OEC)Fe^{II}(NO)]^-$, is located at 1585 cm^{-1} which represents a difference of 182 cm^{-1} between ν_{NO} of the neutral and that of the singly reduced compound. Such a large shift in ν_{NO} is consistent with a change in geometry of the MNO unit upon reduction, i.e, a change from a linear to a bent Fe–N–O arrangement upon going from (OEC)Fe^{III}(NO) to $[(OEC)Fe^{II}(NO)]^-$. Differences in ν_{NO} of 170 to 187 cm^{-1} are also seen between $[(P)Fe^{III}(NO)]^+$ and (P)Fe^{II}(NO) where P = OEP, TPP or TMP (see Table 5). The ν_{NO} values of the iron(II) porphyrins are all higher by 82–93 cm^{-1} than that of the electrogenerated iron(II) corrole, due most likely to the higher negative charge on the corrole macrocycle. However, the controlling factor in the value of $\Delta\nu_{NO}$ seems clearly to be the change from a linear to a bent Fe–N–O configuration upon going from the iron(III) to the iron(II) form of the corrole.

(74) Hoffmann, R.; Chen, M. M. L.; Elian, M.; Rossi, A. R.; Mingos, D. M. P. *Inorg. Chem.* **1974**, *13*, 2666.
(75) Cotton, A. F.; Wilkinson, G. *Advanced Inorganic Chemistry*, 5th ed.; Wiley: New York, 1988.

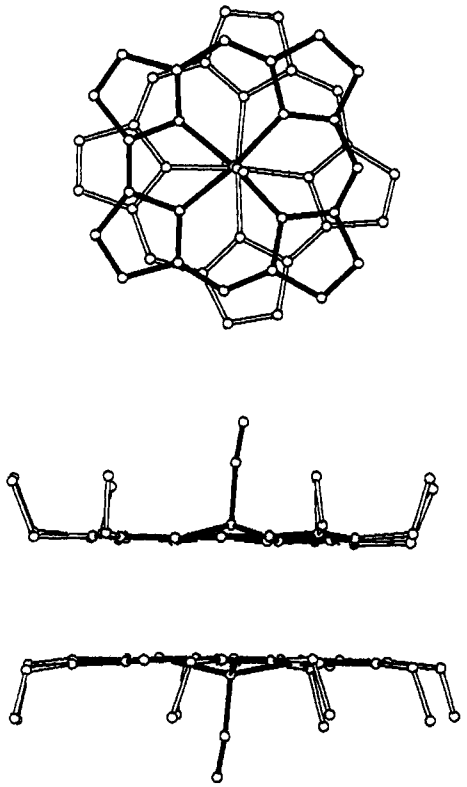

Figure 7. Computer drawn model of the singly oxidized $[(OEC)Fe(NO)]^+ \cdot FeCl_4^-$: (top) upper view (ethyl substituents and hydrogens omitted); (bottom) side view (hydrogens omitted). The interplanar spacing of the two corrole macrocycles is 3.21 Å, while the iron–iron distance is 3.96 Å.

The UV–visible spectroelectrochemical and ESR spectroscopic data indicate that the singly reduced product of $(OEC)Fe^{III}(NO)$ can be formulated as $[(OEC)Fe^{II}(NO)]^-$ and the ESR spectrum is consistent with a five-coordinate iron(II) macrocyclic complex containing a bent MNO unit.[3]

The ESR and UV–visible spectral data are self-consistent and give clear evidence for formation of an iron(III) nitrosyl corrole π-cation radical rather than an iron(IV) nitrosyl corrole upon the first one-electron oxidation of (OEC)Fe(NO). The ν_{NO} band of $[(OEC)Fe^{III}(NO)]^{\bullet+}$ is located at 1815 cm^{-1} which is 48 cm^{-1} higher than the ν_{NO} band of $(OEC)Fe^{III}(NO)$. A similar small change in ν_{NO} is seen upon oxidation of those iron and cobalt porphyrin-like compounds which are oxidized at the macrocycle (see Table 5) and this suggests that a similar assignment can be made upon the conversion of $(OEC)Fe^{III}(NO)$ to $[(OEC)Fe^{III}(NO)]^{\bullet+}$. Neutral (OEC)Fe(NO) contains a linear Fe–N–O unit, and this is also the case for $[(OEC)Fe^{III}(NO)]^{\bullet+}$ as indicated by the X-ray structure shown in Figure 7. Selected X-ray data for the neutral and the oxidized compounds are summarized in Table 7 and Figure 8. $[(OEC)Fe(NO)]^{\bullet+}$ forms a tight π-π dimer with cofacial corrole moities mutually rotated by 132° resulting in the flattening of the corrole ligand. There is almost no lateral shift of the corrole frameworks and the separation of the corrole planes is small (3.21 Å) as is the iron–iron distance (3.96 Å). Similar small distances between the two porphyrin planes of octaethylporphyrin π-cation radicals have been reported (3.19–3.31 Å) for other compounds.[76-78] The N_4-plane distance in the

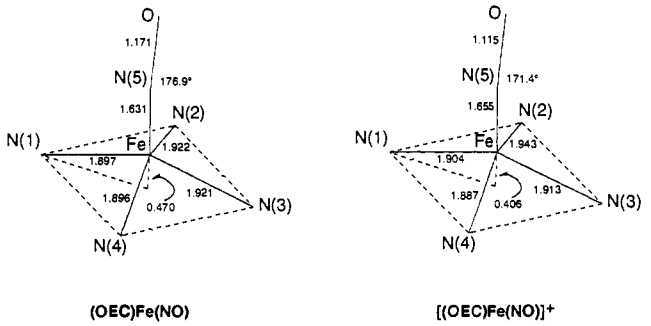

Figure 8. Structural parameters regarding the coordination geometry of the iron atom in (OEC)Fe(NO) and $[(OEC)Fe(NO)]^{\bullet+}$.

π–π dimer is shorter (3.15 Å) than the core–core distance for $[(OEC)Fe(NO)]^{\bullet+}$ and this indicates a displacement of the pyrrole nitrogen atoms toward the other corrole moiety of the dimer due to an attractive interaction. Compared to the starting compound, $[(OEC)Fe(NO)]^{\bullet+}$ shows a distorsion of the corrole ligand leading to slightly irregular Fe–N bond lengths. A comparison of the singly oxidized and neutral nitrosyl derivatives also shows a longer Fe–NO bond (1.655 vs 1.631 Å) and a shorter N–O bond (1.115 vs 1.171 Å) in the oxidized compound, indicating a decreased metal–nitrosyl back-donation due to the lowered electron density at the metal. The iron atom is less displaced from the corrole plane in the case of $[(OEC)Fe(NO)]^{\bullet+}$ (the distance from the N_4 plane and the corrole core being 0.406 and 0.371 Å, respectively) than in the neutral compound (0.470 and 0.556 Å).

Finally, it should be pointed out that $[(OEC)Fe^{III}(NO)]^{\bullet+}$ is the first example where a singly oxidized iron(III) corrole exists as a π-cation radical rather than as a species containing a discrete iron(IV) unit as in the case for (OEC)FeCl, $(OEC)Fe(C_6H_5)$, and $[(OEC)Fe]_2O$.[52]

Summary

To our knowledge, $(OEC)Fe^{III}(NO)$ is the first neutral iron(III) nitrosyl tetrapyrrole to be reported. The complex undergoes three oxidations in both CH_2Cl_2 and PhCN, the first two of which are reversible and occur at the corrole macrocycle to stepwise generate a stable iron(III) π-cation radical and dication both of which still contain a coordinated NO axial ligand. The third oxidation process totally disappears at low temperature or fast scan rates in CH_2Cl_2. Two one-electron reductions of $(OEC)Fe^{III}(NO)$ are also observed by cyclic voltammetry in PhCN, the first of which involves the metal center and generates a stable five-coordinate iron(II) nitrosyl corrole. The second electroreduction was not spectroscopically characterized and no information is available as to the site of electron transfer.

Acknowledgment. The support of the Robert A. Welch Foundation (K.M.K., Grant E-680), the National Institutes of Health, grant number GM25172 (K.M.K.), the Centre National de la Recherche Scientifique (M.G., J.P.G.), the Deutsche Forschungsgemeinschaft (S.W., E.V.), and the University of Houston Energy Laboratory (grant) is gratefully acknowledged. We also acknowledge Dr. Naoto Azuma for help in taking ESR measurements at 77 K.

(76) Scheidt, W. R.; Song, H.; Haller, K. J.; Safo, M. K.; Orosz, R. D.; Reed, C. A.; Debrunner, P. G.; Schulz, C. E. *Inorg. Chem.* **1992**, *31*, 939.
(77) Song, H.; Reed, C. A.; Scheidt, W. R. *J. Am. Chem. Soc.* **1989**, *111*, 6867.
(78) Song, H.; Orosz, R. D.; Reed, C. A.; Scheidt, W. R. *Inorg. Chem.* **1990**, *29*, 4274.